Geophysical Research Letters

RESEARCH LETTER
10.1029/2019GL085617

Asian Winter Monsoon Imprint on Holocene SST Changes at the Northern Coast of the South China Sea

Yancheng Zhang[1], Kai Zhu[1], Chao Huang[2], Deming Kong[3], Yuxin He[4], Huanye Wang[5], Weiguo Liu[5], Zhouqing Xie[6], Gangjian Wei[2], and Zhonghui Liu[1]

[1]Department of Earth Sciences, University of Hong Kong, Hong Kong, SAR China, [2]State Key Laboratory of Isotope Geochemistry, Guangzhou Institute of Geochemistry, Chinese Academy of Sciences, Guangzhou, China, [3]Guangdong Province Key Laboratory for Coastal Ocean Variation and Disaster Prediction, Guangdong Ocean University, Zhanjiang, China, [4]School of Earth Sciences, Zhejiang University, Hangzhou, China, [5]State Key Laboratory of Loess and Quaternary Geology, Institute of Earth Environment, Chinese Academy of Sciences, Xi'an, China, [6]School of Earth and Space Science, University of Science and Technology of China, Hefei, China

Abstract Independent inference of the Asian winter monsoon (AWM), albeit achieved at several sparse sites, has reached no consensus for its variability through the Holocene. A sediment core from the northern coast of the South China Sea (SCS) was utilized to analyze organic biomarkers at (bi-)decadal resolution, unveiling how SCS oceanic conditions fingerprint the AWM signal. Generally, alkenone sea surface temperature (SST) record, resembling the temporal structures of integrated tropical SST over the past 7,500 years, shows abnormal cool temperatures (up to ~4 °C) during the Little Ice Age and between ~1,200 and 2,500 years BP, when windborne terrigenous hopane compounds experienced considerable increases superimposed on a general increasing trend. Our results, together with augmented SST gradient between the SCS coast and open ocean, consistently suggest AWM strengthening toward the late Holocene. An intensified AWM during cold intervals like the Little Ice Age would have provided strong positive feedback to enhance coastal cooling.

Plain Language Summary Reconstructions of the Holocene Asian winter monsoon (AWM) history from terrestrial proxies are not only limited but also opposite, with both strengthening and weakening trends as reported. This study sheds additional insight into this controversy by analyzing the organic geochemistry of a sediment core at the northern coast of the South China Sea, where oceanic conditions such as sea surface temperature intensively interact with the AWM. We observed substantial surface cooling and a remarkable increase in terrestrial-sourced hopane content concurrently toward the late Holocene, with the maximum taking place during the Little Ice Age and between 1,200 and 2,500 years ago. Together with enhanced temperature contrast between the coast and open ocean, our results clearly demonstrate an overall intensification of the Holocene AWM toward the present, antiphased with Asian summer monsoon changes.

Key Points:
- Bi-decadal alkenone SST changes at the northern SCS coast over the past ~7,500 years
- Sharp increase in flux of terrestrial-sourced hopane compounds during cool intervals
- Strengthened winter monsoon toward the late Holocene, particularly at the LIA

Supporting Information:
- Supporting Information S1

Correspondence to:
Z. Liu,
zhliu@hku.hk

Citation:
Zhang, Y., Zhu, K., Huang, C., Kong, D., He, Y., Wang, H., et al (2019). Asian winter monsoon imprint on Holocene SST changes at the northern coast of the South China Sea. *Geophysical Research Letters*, *46*, 13,363–13,370. https://doi.org/10.1029/2019GL085617

Received 29 SEP 2019
Accepted 11 NOV 2019
Accepted article online 13 NOV 2019
Published online 22 NOV 2019

1. Introduction

Despite the fundamental role played by the Asian winter monsoon (AWM) in the climate system, its long-term variability, particularly during the Holocene (since ~11,500 years before present, years BP hereafter), is only poorly understood to date. Because the divergence of dry air from the Siberia-Mongolia continent enables the AWM to effectively redistribute a massive amount of aeolian dust and aerosol in boreal cold months (Bollasina et al., 2011; Li et al., 2016), analyses of grain size, mineralogical, and geochemical proxies from Chinese loess deposits are commonly carried out to determine AWM intensity (Kang et al., 2018; Li & Morrill, 2015; Stevens et al., 2007). Paleorecords at these individual sites are helpful to offer important insight into AWM evolution, but collectively, they point out controversies in terms of not only general AWM structures over the Holocene but also multicentennial to millennial scale variations within this specific interval (Hao et al., 2012; Li & Morrill, 2015; Kang et al., 2018; Xia et al., 2014). Furthermore, at Huguangyan Maar Lake near the northern coast of the South China Sea (SCS), opposite temporal features of Holocene AWM strength have been inferred from magnetic susceptibility/the S ratio (Yancheva et al., 2007) and diatom assemblages (Wang et al., 2012), whereas climate model simulations tend to support the diatom view of a weakening AWM toward the present (Wen et al., 2016). As such, additional evidence of

AWM variability over the Holocene, based on a variety of reliable indicators, is essential to scrutinize its behavior and then to evaluate the coupling relationship with the Asian summer monsoon (ASM) (An et al., 2012; Wang et al., 2017; Wen et al., 2016).

The SCS is strongly involved in ocean-atmosphere processes of the Asian monsoon system (Lau & Nath, 2009; Wang et al., 2009) and is thus well suited to decipher the AWM signal. In fact, proxy-based temperature reconstructions in the SCS indicate thermal differences in both the horizontal and vertical directions, revealing a stronger AWM during cold intervals of the last deglaciation (Huang et al., 1997, 2011; Steinke et al., 2011; Tian et al., 2010). Relative to the coarse resolution (>~200 year per sample) of those sediment cores in the open ocean, recent work has shown that sea surface temperature (SST) changes at the northern coast of the SCS, which are sensitive to the prevailing winds in different seasons (Figure 1), are quite promising for manifesting AWM strength in a detailed manner (Kong, 2014). This concept was first verified in a pilot study by Kong et al. (2014), who used an SST gradient between two core sites, HKUV16 (22°17′N, 113°52′E) and NS02G (20°10′N, 115°16′E), to corroborate a gradually intensified AWM after ~7,000 years BP. Unfortunately, the large chronological uncertainty of core HKUV16 and human disturbance on its core-top sediment (Kong et al., 2014) hinder a closer look into how centenary to millennial scale AWM changes affect SCS coastal conditions. This knowledge gap is filled here by a well-dated marine sediment core YJ, retrieved ~200 km to the southwest of the Pearl River estuary in the northern SCS (Figure 1).

We conducted biomarker analyses of the new core YJ from the inner continental shelf with a high sedimentation rate (Figure 1). In this respect, long-chain unsaturated alkenones ($U^{K'}_{37}$) and hopanoid compounds were employed as a paleothermometer (Prahl et al., 1988) and tracer of terrigenous biomass input (Xie et al., 2013), respectively. Paired variations of these records, with bidecadal resolution over the past ~7,500 years, allow a clear understanding of Holocene AWM variability through its impact on the SCS coast. Our biomarker results from the coast, in addition to an identified enhanced SST gradient between the SCS coast and open ocean in the late Holocene, effectively suggest an intensification of the Holocene AWM.

2. Materials and Methods

2.1. Core Site

The 839-cm-long sediment core YJ (112°8.08′E, 21°31.44′N, ~21-m water depth) was collected largely outside of the Pearl River freshwater effect. At this site, available data sets AVHRR 1985-2006 (Casey, 2013) and CSIRO Atlas of Regional Seas CARS2009 (Dunn & Ridgway, 2002) exhibit prominent seasonal variations in SST (~29 °C in June–August and ~20 °C in December–February; Figure 1) and slight changes in sea surface salinity (~32.8 psu in June–August and ~33.4 psu in December–February). In contrast to sediment core HKUV16, this site bears multiple times of magnitude smaller sea surface salinity differences between summer and winter (Jiang & Wang, 2018), thus impressing minor (if any) influence of the Pearl River freshwater. Seasonal temperatures of the water column along the northern coast of the SCS highlight shore-parallel gradients and strong vertical mixing in winter, while horizontal homogenization and vertical stratification in summer (Figure 1; Jing et al., 2009; Wang, 2007). Unlike the coastal regions to the east of the Pearl River delta and to the northeast of Hainan Island, this site experiences little summer upwelling effect (evidenced by the absence of a ~0.5 °C cooling signal; Figure 1b). Meanwhile, based on modern observations, the AWM index (Ding et al., 2014) is negatively correlated with winter SST at the study site over the past ~40 years, showing weakened AWM and relatively warm winter SST around 1990s (supporting information Figures 1 and 2). Altogether, sediment core YJ is ideal to document past AWM changes.

Based on a combination of 13 lead (^{210}Pb)/cesium (^{137}Cs) and 18 radiocarbon (^{14}C) dates, the age model for the upper 610 cm of our core YJ covers the past ~7,500 years. Particularly, these age control points were operated within the R script BACON software, incorporating a total of 10,000 age-depth realizations, to calculate the mean age and also the 2σ analytical uncertainty at 1-cm resolution (Figure S3). The derived chronology has been reported previously in Huang et al. (2018), and fully described in supporting information.

2.2. Biomarkers

The core YJ, situated on a modern mud belt formed predominantly by Pearl River sediment discharge (Liu et al., 2014), consists of fine-grained muddy sediment with grey clay and/or clayey silt. Downcore results of lithology, grain size and chronology (Figure S3), as presented in Huang et al. (2018), collectively suggest that

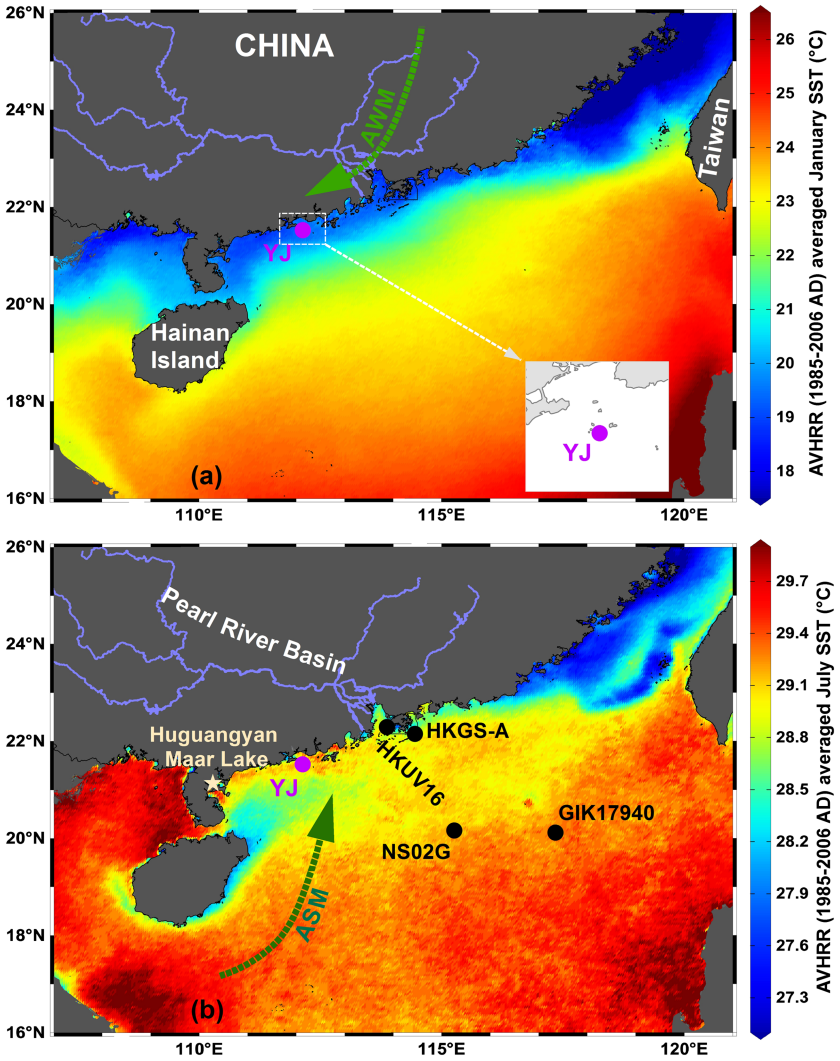

Figure 1. Location of site YJ (pink dot) and published records in the northern South China Sea (black dots) and at Huguangyan Maar Lake (yellow star). The color scale shows long-term average January (a) and July (b) sea surface temperatures (SSTs) from the AVHRR data set (Casey, 2013), and the green dashed arrows sketch the dominant vectors of corresponding surface winds.

the sedimentary sequence is neither physically nor biologically disturbed and is suitable to investigate past ocean-atmosphere-land interactions on longer timescales. To generate downcore biomarker records, we sampled core YJ in steps of 1 cm for the upper 190 cm and then 2 cm down to its bottom. Such sampling steps, based on our age model (supporting information), permitted resolution of ~10–25 year per sample, except for ~80 year per sample at 60- to 80-cm depth. Bulk sediment samples (~5 g) were dried, powdered, and soaked to extract total lipids with dichloromethane (DCM) solvent: methanol (MeOH) (9:1; v/v) in 60 ml vials under ultrasonic waves in a 40 °C water bath for three cycles (~15 min each). The extract was hydrolyzed by 6% KOH in MeOH to remove alkenoates and then separated into three fractions by silica gel column chromatography using eluents of *n*-hexane, DCM, and MeOH. Finally, alkenones were kept in the DCM fraction, and hopanes were kept in the hexane fraction.

2.2.1. Alkenones ($U^{K'}_{37}$)

We analyzed long-chain alkenones following a procedure from Kong et al. (2014) and He et al. (2014). Measurements of the alkenone fraction were carried out on an Agilent 7890 gas chromatograph (GC) equipped with a flame ionization detector. An internal standard of *n*-C_{36} alkane was added repeatedly for every 20 samples to quantify alkenones. The $U^{K'}_{37}$ ratio was obtained via an equation from Prahl et al.

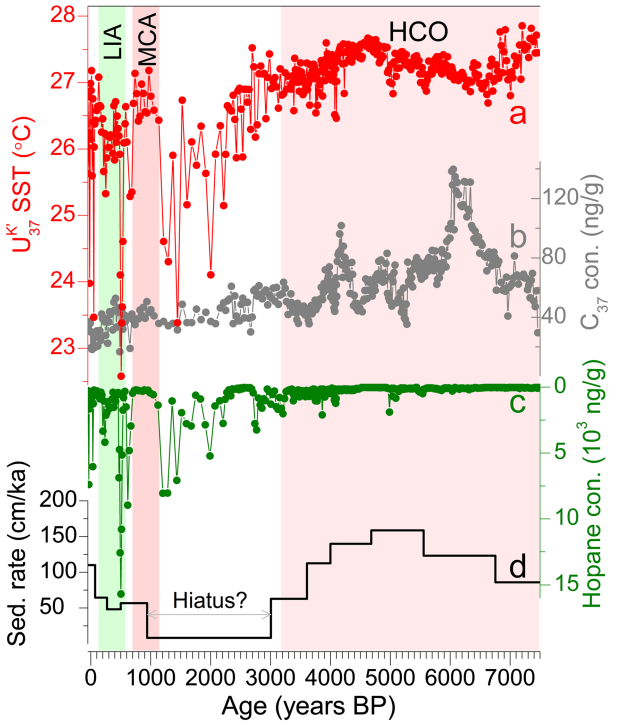

Figure 2. Downcore geochemical proxies of sediment core YJ over the past 7,500 years, including (a) $U^{K'}_{37}$-SST record, (b) C_{37} concentration, (c) total hopane concentration (reversed scale), and (d) sedimentation rate. The color bars represent three key intervals discussed in the text, for example, the Holocene Climate Optimum (HCO, before ~3,500 years BP), Medieval Climate Anomaly (MCA, ~700–1100 years BP) (red), and Little Ice Age (LIA, ~150–550 years BP) (green).

(1988): $U^{K'}_{37} = C_{37:2}/(C_{37:2} + C_{37:3})$, where $C_{37:2}$ and $C_{37:3}$ are the concentrations of diunsaturated and triunsaturated C_{37} alkenones, respectively. The mean annual SST was calculated by the following equation: SST = $(U^{K'}_{37} - 0.092)/0.031$, which was developed specifically for the SCS (Pelejero & Grimalt, 1997). Analytical uncertainties were typically less than 0.005 unit for the $U^{K'}_{37}$ ratio (equivalent to ~0.2 °C for an SST estimate) and 5% for the C_{37} concentration. Below 610 cm, alkenone concentration is generally low (<10 ng/g) and thus not presented here.

2.2.2. Hopanoids

Hopane compounds in the hexane fraction were identified by the Agilent 7890 GC equipped with mass spectrometry and subsequently quantitatively determined by the 7890 GC-flame ionization detector (He et al., 2015, and references therein). The GC temperature protocol was set as follows: 60 (1 min) to 250 °C at a rate of 20 °C/min, 250 to 270 °C at a rate of 5 °C/min, 270 to 310 °C at a rate of 2 °C/min and ultimately maintained at 310 °C for 15 min. Direct comparisons of peak areas with a *n*-C_{36} alkane standard of known concentration were drawn to quantify different hopane components. Finally, the total hopane concentration was obtained by adding those of the major C_{29}-C_{31} αβ hopanes together.

3. Results

The $U^{K'}_{37}$-SST record of core YJ fluctuates between 22 and 28 °C over the past ~7,500 years, displaying a long-term cooling trend with augmented SST variability (Figure 2a). Generally, higher values occurred before about 3,500 years BP (27.2 ± 0.3 °C, also note a slight depression from 5,000 to 7,000 years BP), during 700–1,100 years BP (the Medieval Climate Anomaly, MCA, 26.7 ± 0.2 °C) and after ~100 years BP, and lower values prevailed during 1,200–2,500 years BP (26.0 ± 0.8 °C) and 150–550 years BP (the Little Ice Age, LIA, 25.7 ± 0.9 °C). It appears that substantial cooling started to take place approximately 2,000–3,000 years BP, while our SST record was relatively coarsely resolved between ~1,200 and 2,500 years BP (owing to lower sedimentation rates or even possible hiatus; Figure 2d). Additionally, the C_{37} alkenone concentration mainly varies from ~30 to 80 ng/g, except for a considerable increase centered at around 6,000 years BP (Figure 2b). In contrast, variations in total hopane concentration characterize a long-term increasing trend with increments of amplitude toward the present (Figure 2c). During warm intervals, for instance, the MCA, total hopane concentration remained quite low, at approximately the same level as earlier than ~3,500 years BP (the Holocene climate optimum, HCO), while a marked increase (2 to 4 orders of magnitude higher) occurred during cool intervals, for example, ~1,200–2,500 years BP and the LIA, with the maximal concentration at the onset of the LIA.

4. Discussion

4.1. SST and Hopane Variations Linked to AWM Intensity

The $U^{K'}_{37}$-SST value of the uppermost sample (25.6 °C) is slightly higher than the composite in situ mean annual SST (24.9 °C) from the AVHRR data set (Figure 1). A similar difference (about 0.8 °C) has also been reported in a few published cores from the northern SCS (Kong et al., 2014), but accurate calculation remains difficult, as the $U^{K'}_{37}$-SST relationship for SCS coastal settings is not established. Since the alkenone unsaturation ratio is calibrated to the mean annual SST, we interpret that $U^{K'}_{37}$-SST values, despite being biased toward summer signals, represent the mean annual SST. Moreover, a set of modern surveys show that, in surface waters of the northern SCS, long-chain alkenones are primarily synthesized by species *Gephyrocapsa oceanica* and *Emiliania huxleyi* in cold months when northeasterly winds prevail (Chen et al., 2007). Further, taking into account that the effect of significant cooling is maintained in wintertime in this particular geographic setting (Figure 1), SST changes in the alkenone record thus would also

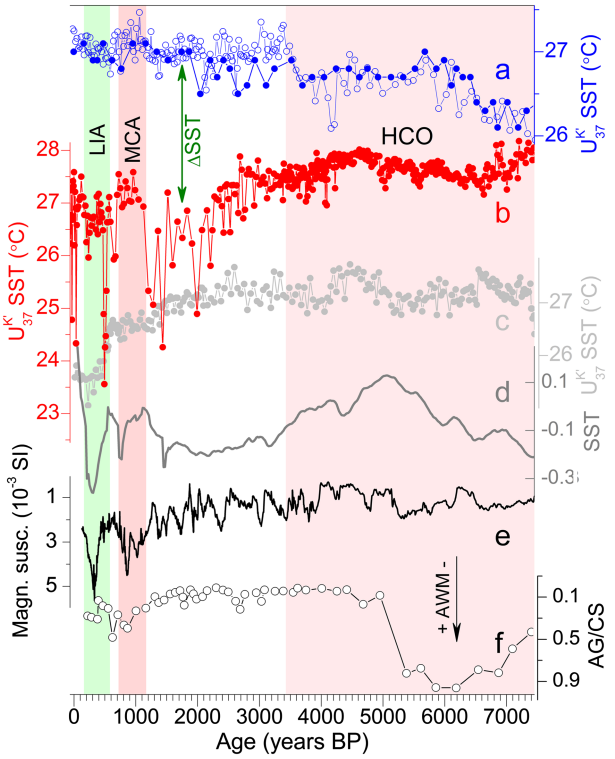

Figure 3. Comparison of $U^{K'}_{37}$-SST records of sediment cores (a) GIK17940 (blue dots) (Wang et al., 1999) and NS02G (blue cycles) (Kong, 2014), (b) YJ (this study), and (c) HKUV16 (Kong et al., 2014), (d) integrated SST anomaly over global tropical coasts (Marcott et al., 2013) as well as (e) magnetic susceptibility (values increase downward, Yancheva et al., 2007) and (f) diatom AG/CS ratio (*A. granulate*/*C. stelligera*; Wang et al., 2012) at Huguangyan Maar Lake. The color bars mark the same intervals as in Figure 2, and the green arrow line denotes the SST gradient between the SCS northern coast and open ocean.

contain a strong winter component. Indeed, Pelejero and Grimalt (1997) suggested that core-top $U^{K'}_{37}$ values in the SCS have a relationship with winter SST as good as that with mean annual SST. However, as alkenones are produced within all seasons and changes in $U^{K'}_{37}$ values could be mainly driven by either winter (Kong et al., 2014; Zhang et al., 2019) or summer (Kong et al., 2015; Lee et al., 2019; Zhang et al., 2013) signals, depending on specific oceanic settings, we prefer to use mean annual calibration (Pelejero & Grimalt, 1997) but also emphasize the more important role of winter temperatures at our study site (Figures S1 and S2). Finally, different equations yield great similarity in the temporal patterns of SST records (e.g., the remarkable cooling of the LIA, not shown) and thereby do not affect our main conclusions.

Substantial decreases of up to ~4 °C during cool intervals, for example, LIA and ~1,200–2,500 year BP in our SST record (Figure 2a), appear to be abnormally high compared with ~1–2 °C cooling at the same intervals across the open ocean of the northern SCS and western tropical Pacific (Chen et al., 2018; Lin et al., 2006; Oppo et al., 2009). Although tropical climate (e.g., El Niño–Southern Oscillation) modulates SST over the northern SCS, the small range out of which (~0.2 °C as observed from instrumental data sets) strongly excludes a major role of El Niño–Southern Oscillation variability in such a large amplitude of cooling at our site. We recognize that along the northern coast of the SCS, surface cooling and intensive vertical mixing, triggered by northeasterly winds, greatly reduce winter SST today (Figures 1a, S1, and S2), but in summer, the southwesterly winds-induced upwelling causes cooler SST only in mosaic regions outside of our study site, for example, to the east of the Pearl River mouth and northeast of Hainan Island (Figure 1b). On this basis, the considerable cooling in these two cold intervals in our case probably results from an extra superimposition of enhanced impact from AWM-related vertical mixing and/or atmospheric cooling. Accordingly, downcore SST variations during the past ~7,500 years, within a range of long-term average winter and summer limits (Figure 2a), can be used to infer the Holocene AWM variability.

In addition, the total hopane concentration experiences pulse-like increases (2 to 4 orders of magnitude higher) during the same cool intervals (Figure 2c). Simultaneously, large differences in sedimentation rates (Figure 2d) and terrigenous organic matter (Huang et al., 2018) between the LIA and ~1,200–2,500 years BP, together with a weakened ASM substantiated by numerous terrestrial records (Liu et al., 2015; Wang et al., 2005), enable us to reject the lateral transport of riverine input as the dominant source of increased hopane compounds. Detailed identification of corresponding samples in these two cool intervals further confirms that hopane compounds, mainly comprising C_{30}-17α(H)21β(H) and C_{31}-17α(H)21β(H)-S, contain little hopene content. Thus, the dramatically high hopane concentrations, a feature not shown in alkenone contents (Figure 2b), are very unlikely to originate from in situ biological production (Pearson et al., 2009; Peters et al., 2005). Rather, an enhanced influx of terrestrial-sourced biomass plausibly acts as a reasonable explanation (He et al., 2015; Xie et al., 2013) because AWM strengthening during cool intervals promoted northeasterly winds, which would transport more terrigenous hopanes from the continent to the northern coast of the SCS (Figure 1a). Conversely, the co-occurrence of increased SST and lower hopane concentrations at our study site implies a reduction in the AWM during warm intervals, for example, the MCA and HCO. Together, our SST and hopane records effectively reflect variations in Holocene AWM intensity, which, in general, intensified toward the present.

4.2. Variations of AWM Intensity During the Past ~7,500 Years

One might argue that a stronger ASM is also able to boost coastal upwelling in the northern SCS (Figure 1b), for example, to the east of the Pearl River delta (Kong et al., 2015; Lee et al., 2019) and northeast of Hainan

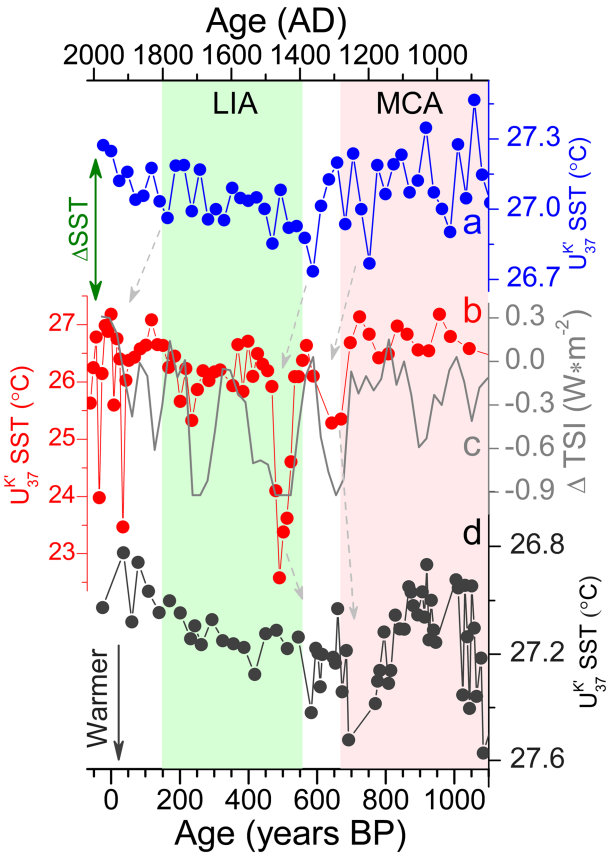

Figure 4. Comparison of $U^{K'}_{37}$-SST records over the last millennium in sediment cores (a) NS02G (Kong et al., 2017), (b) YJ (this study), and (d) HKGS-A (higher values downward) (Lee et al., 2019). The color bars and green arrow line outline the same intervals and SST gradient, respectively, as in Figure 3, and the dashed gray lines hint at the correspondence of three independent records within their chronological uncertainties. Total solar irradiance (TSI) (Steinhilber et al., 2009) is also superimposed upon the SST record (c). Note different temperature scale used for the three records.

Island (Jiang & Wang, 2018; Jing et al., 2009). This hypothesis, if applicable to our case, is possible to explain lower SST but hard to reconcile with exceptionally high hopane concentrations. The reason behind this is that the prevailing southwesterly winds, activated along with the ASM, are apparently reversed in direction to deliver land-sourced biomass toward the northern coast of the SCS (Figure 1b). In addition, the postulated ASM enhancement over these cool intervals also contradicts a growing body of compelling evidence in line with a weakened ASM for the same time slices (Hu et al., 2008; Lee et al., 2019; Wang et al., 2005). Instead, variations in AWM strength could feasibly explain our multiple proxy records for both cold and warm intervals from multicentennial to millennial scales. It is worth stressing that despite opposite reconstructions of the Holocene AWM at Huguangyan Maar Lake, our results agree with that inferred from the magnetic susceptibility/S ratio (Yancheva et al., 2007; Figure 3e) but differ from the one based on diatom assemblages (Wang et al., 2012; Figure 3f) and the simulated Holocene AWM (Wen et al., 2016).

The last millennium, in which both the LIA and MCA emerged as climate anomalies (Mann et al., 2008), is an excellent time window to disentangle the spatial structures of how northern SCS coastal conditions interact with the Asian monsoon system (Figure 4). Our recent work on another sediment core HKGS-A, in the southeast waters offshore of Hong Kong (Figure 1b) actually revealed the impact of summer monsoon-driven upwelling on coastal SST changes in the northern SCS (Lee et al., 2019). It is evident that the ASM cooling effect outweighed the original signal of global temperature change, resulting in relatively warm SST during the LIA and cool conditions during the MCA (Figure 4d). In contrast, the SST record in core YJ exhibits inherent features of the LIA and MCA but with larger amplitude of SST changes (Figure 4b) and HCO as well, following the typical temporal characteristics of integrated tropical SST anomaly (Figures 3b and 3d) (Marcott et al., 2013). Such discrepancies in the temporospatial patterns of SST changes across the SCS coastal upwelling regions (Figures 4b and 4d) thus further consolidate the dominant imprint of the AWM-induced cooling effect at our study site YJ, as it does today.

On longer timescales, coastal SST records in both core YJ and existing core HKUV16 show marked warm conditions during the HCO (Figures 3b and 3c). This is in striking contrast to previously published SST records from the SCS open ocean that, for instance, cores NS02G and GIK17940 (Figure 3a), witnessed relatively cool HCO conditions (Lin et al., 2006; Oppo & Sun, 2005; Wang et al., 1999; Wei et al., 2007; Zhou et al., 2012). Clearly, the SST difference between sites YJ and NS02G/GIK17940 (Figures 3a and 3b), a measure of thermal contrast between the SCS northern coast and open ocean (Kong et al., 2014), again reinforces an intensification of the AWM toward the late Holocene. We note that this notion also works well for the last millennium since an increased temperature gradient between the open ocean and coast is evident during the LIA (particularly at its onset; Figures 4a and 4b), signaling a strengthened AWM. Furthermore, in-phase covariations in the SST record in core YJ and total solar irradiance (Steinhilber et al., 2009) also underline the possible control of external forcing on AWM intensity (Fig. 4c), which deserves more effort (e.g., climate models) in the future.

5. Conclusion

We have reconstructed $U^{K'}_{37}$-based SST changes, along with hopane contents, over the past 7,500 years from a sediment core drilled at the northern coast of the SCS. The $U^{K'}_{37}$-SST record shows warm conditions during the HCO and MCA and remarkably cool temperatures during the LIA. In addition, hopane compounds exhibit

high extremes during cool intervals, such as the LIA. These proxy records together facilitate the coupled dynamics between northern SCS coastal conditions and AWM variations from multicentennial to millennial timescales and strongly indicate a long-term strengthening trend of the Holocene AWM toward the present, with significant intensification during cool climate intervals, thus opposite to ASM changes. We further suggest that SST changes at the northern coast of the SCS are considerably amplified by the AWM cooling effect, and hence, the SST difference between the coast and open ocean could effectively capture the Holocene AWM intensity.

Acknowledgments
We sincerely thank the editor and two anonymous referees who provided insightful comments and suggestions to improve our manuscript. This work was supported by the National Key Research and Development Program of China (2016YFA0601204) and HK RGC grant 17325516. All the data presented in this paper are accessible via the PANGAEA database (doi:10.1594/PANGAEA.905642).

References

An, Z., Colman, S., Zhou, W., Li, X., Brown, E., Jull, A., et al. (2012). Interplay between the Westerlies and Asian monsoon recorded in Lake Qinghai sediments since 32 ka. *Scientific Reports*, *2*, 1–7.

Bollasina, M., Ming, Y., & Ramaswamy, V. (2011). Anthropogenic aerosols and the weakening of the South Asian summer monsoon. *Science*, *334*(6055), 502–505. https://doi.org/10.1126/science.1204994

Casey, K. (2013). US DOC/NOAA/NESDIS > National Oceanographic Data Center, AVHRR Pathfinder version 5.0 global 4 km sea surface temperature (SST) cloud-screened monthly climatologies for 1985-2006 (NODC Accession 0110657). Version 1.1. National Oceanographic Data Center, NOAA.

Chen, T., Cobb, K. M., Roff, G., Zhao, J., Yang, H., Hu, M., & Zhao, K. (2018). Coral-derived western Pacific tropical sea surface temperatures during the last millennium. *Geophysical Research Letters*, *45*, 3542–3549. https://doi.org/10.1002/2018GL077619

Chen, Y., Chen, H., & Chung, C. (2007). Seasonal variability of coccolithophore abundance and assemblage in the northern South China Sea. *Deep-Sea Research Part II*, *54*, 1617–1633.

Ding, Y., Liu, Y., Liang, S., Ma, X., Zhang, Y., Si, D., et al. (2014). Interdecadal variability of the East Asian winter monsoon and its possible links to global climate change. *Journal of Meteorological Research*, *28*(5), 693–713.

Dunn, J., & Ridgway, K. (2002). Mapping ocean properties in regions of complex topography. *Deep-Sea Research Part I*, *49*, 591–604.

Hao, Q., Wang, L., Oldfield, F., Peng, S., Qin, L., Song, Y., et al. (2012). Delayed build-up of Arctic ice sheets during 400,000-year minima in insolation variability. *Nature*, *490*(7420), 393–396. https://doi.org/10.1038/nature11493

He, Y., Zhao, C., Zheng, Z., Liu, Z., Wang, N., Li, J., & Cheddadi, R. (2015). Peatland evolution and associated environmental changes in central China over the past 40,000 years. *Quaternary Research*, *84*, 255–261.

He, Y., Zhou, X., Liu, Y., Yang, W., Kong, D., Sun, L., & Liu, Z. (2014). Weakened Yellow Sea Warm Current over the last 2–3 centuries. *Quaternary International*, *349*, 252–256.

Hu, C., Henderson, G., Huang, J., Xie, S., Sun, Y., & Johnson, K. (2008). Quantification of Holocene Asian monsoon rainfall from spatially separated cave records. *Earth and Planetary Science Letters*, *266*, 221–232.

Huang, C., Liew, P., Zhao, M., Chang, T., Kuo, C., Chen, M., et al. (1997). Deep sea and lake records of the Southeast Asian paleomonsoons for the last 25 kyrs. *Earth and Planetary Science Letters*, *146*, 59–72.

Huang, C., Zeng, T., Ye, F., Xie, L., Wang, Z., Wei, G., et al. (2018). Natural and anthropogenic impacts on environmental changes over the past 7500 years based on the multi-proxy study of shelf sediments in the northern South China Sea. *Quaternary Science Reviews*, *197*, 35–48.

Huang, E., Tian, J., & Steinke, S. (2011). Millennial-scale dynamics of the winter cold tongue in the southern South China Sea over the past 26 ka and the East Asian winter monsoon. *Quaternary Research*, *75*, 196–204.

Jiang, R., & Wang, Y. (2018). Modeling the ecosystem response to summer coastal upwelling in the northern South China Sea. *Oceanologia*, *60*, 32–51.

Jing, Z., Qi, Y., Hua, Z., & Zhang, H. (2009). Numerical study on the summer upwelling system in the northern continental shelf of the South China Sea. *Continental Shelf Research*, *29*, 467–478.

Kang, S., Wang, X., Roberts, H., Duller, G., Cheng, P., Lu, Y., & An, Z. (2018). Late Holocene anti-phase change in the East Asian summer and winter monsoons. *Quaternary Science Reviews*, *188*, 28–36.

Kong, D. (2014). Climatic changes in the northern South China Sea since the last glacial maximum. PhD Thesis. University of Hong Kong, https://doi.org/10.5353/th_b5312314.

Kong, D., Tse, Y., Jia, G., Wei, G., Chen, M., Zong, Y., & Liu, Z. (2015). Cooling trend over the past 4 centuries in northeastern Hong Kong waters as revealed by alkenone-derived SST records. *Journal of Asian Earth Sciences*, *114*, 497–503.

Kong, D., Wei, G., Chen, M., Peng, S., & Liu, Z. (2017). Northern South China Sea SST changes over the last two millennia and possible linkage with solar irradiance. *Quaternary International*, *459*, 29–34.

Kong, D., Zong, Y., Jia, G., Wei, G., Chen, M.-T., & Liu, Z. (2014). The development of late Holocene coastal cooling in the northern South China Sea. *Quaternary International*, *349*, 300–307.

Lau, N., & Nath, M. (2009). A model investigation of the role of air-sea interaction in the climatological evolution and ENSO-related variability of the summer monsoon over the South China Sea and Western North Pacific. *Journal of Climate*, *22*, 4771–4792.

Lee, W., Poon, K., Kong, D., Sewell, R., Zong, Y., Zhang, Y., & Liu, Z. (2019). Summer monsoon-induced upwelling dominated coastal SST variations in the northern South China Sea over the last two millennia. *The Holocene*, *29*, 691–698.

Li, Y., & Morrill, C. (2015). A Holocene East Asian winter monsoon record at the southern edge of the Gobi Desert and its comparison with a transient simulation. *Climate Dynamics*, *45*, 1219–1234.

Li, Z., Lau, W., Ramanathan, V., Wu, G., Ding, Y., Manoj, M., et al. (2016). Aerosol and monsoon climate interactions over Asia. *Reviews of Geophysics*, *54*, 866–929. https://doi.org/10.1002/2015RG000500

Lin, D., Liu, C., Fang, T., Tsai, C., Murayama, M., & Chen, M. (2006). Millennial-scale changes in terrestrial sediment input and Holocene surface hydrography in the northern South China Sea (IMAGES MD972146). *Palaeogeography Palaeoclimatology Palaeoecology*, *236*, 56–73.

Liu, J., Chen, J., Zhang, X., Li, Y., Rao, Z., & Chen, F. (2015). Holocene East Asian summer monsoon records in northern China and their inconsistency with Chinese stalagmite $\delta^{18}O$ records. *Earth Science Reviews*, *148*, 194–208.

Liu, Y., Gao, S., Wang, Y., Yang, Y., Long, J., Zhang, Y., & Wu, X. (2014). Distal mud deposits associated with the Pearl River over the northwestern continental shelf of the South China Sea. *Marine Geology*, *347*, 43–57.

Mann, M., Zhang, Z., Hughes, M., Bradley, R., Miller, S., Rutherford, S., & Ni, F. (2008). Proxy-based reconstructions of hemispheric and global surface temperature variations over the past two millennia. *Proceedings of the National Academy of Sciences of the United States of America*, *105*(36), 13252–13257. https://doi.org/10.1073/pnas.0805721105

Marcott, S., Shakun, J., Clark, P., & Mix, A. (2013). A reconstruction of regional and global temperature for the past 11,300 years. *Science*, *339*(6124), 1198–1201. https://doi.org/10.1126/science.1228026

Oppo, D. W., Rosenthal, Y., & Linsley, B. (2009). 2,000-year-long temperature and hydrology reconstructions from the Indo-Pacific warm pool. *Nature*, *460*(7259), 1113–1116. https://doi.org/10.1038/nature08233

Oppo, D. W., & Sun, Y. (2005). Amplitude and timing of sea-surface temperature change in the northern South China Sea: Dynamic link to the East Asian monsoon. *Geology*, *33*, 785–788.

Pearson, A., Leavitt, W., Sáenz, J., Summons, R., Tam, M., & Close, H. (2009). Diversity of hopanoids and squalene-hopene cyclases across a tropical land-sea gradient. *Environmental Microbiology*, *11*(5), 1208–1223. https://doi.org/10.1111/j.1462-2920.2008.01817.x

Pelejero, C., & Grimalt, J. (1997). The correlation between the $U^{K'}_{37}$ index and sea surface temperatures in the warm boundary: The South China Sea. *Geochimica et Cosmochimica Acta*, *61*, 4789–4797.

Peters, K., Walters, C., & Moldowan, J. (2005). *The biomarker guide* (p. 490). Cambridge: Cambridge University Press.

Prahl, F., Muehlhausen, L., & Zahnle, D. (1988). Further evaluation of long-chain alkenones as indicators of paleoceanographic conditions. *Geochimica et Cosmochimica Acta*, *52*, 2303–2310.

Steinhilber, F., Beer, J., & Fröhlich, C. (2009). Total solar irradiance during the Holocene. *Geophysical Research Letters*, *36*, L19704. https://doi.org/10.1029/2009GL040142

Steinke, S., Glatz, C., Mohtadi, M., Groeneveld, J., Li, Q., & Jian, Z. (2011). Past dynamics of the East Asian monsoon: No inverse behaviour between the summer and winter monsoon during the Holocene. *Global and Planetary Change*, *78*, 170–177.

Stevens, T., Thomas, D., Armitage, S., Lunn, H., & Lu, H. (2007). Reinterpreting climate proxy records from late Quaternary Chinese loess: A detailed OSL investigation. *Earth Science Reviews*, *80*, 111–136.

Tian, J., Huang, E., & Pak, D. (2010). East Asian winter monsoon variability over the last glacial cycle: Insights from a latitudinal sea-surface temperature gradient across the South China Sea. *Palaeogeography Palaeoclimatology Palaeoecology*, *292*, 319–324.

Wang, B., Huang, F., Wu, Z., Yang, J., Fu, X., & Kikuchi, K. (2009). Multi-scale climate variability of the South China Sea monsoon: A review. *Dynamics of Atmospheres and Oceans*, *47*, 15–37.

Wang, L., Li, J., Lu, H., Gu, Z., Rioual, P., Hao, Q., et al. (2012). The East Asian winter monsoon over the last 15,000 years: Its links to high-latitudes and tropical climate systems and complex correlation to the summer monsoon. *Quaternary Science Reviews*, *32*, 131–142.

Wang, L., Sarnthein, M., Erlenkeuser, H., Grootes, P. M., Grimalt, J. O., Pelejero, C., & Linck, G. (1999). Holocene variations in Asian monsoon moisture: A bidecadal sediment record from the South China Sea. *Geophysical Research Letters*, *26*, 2889–2892.

Wang, P., Wang, B., Cheng, H., Fasullo, J., Guo, Z., Kiefer, T., & Liu, Z. (2017). The global monsoon across time scales: Mechanisms and outstanding issues. *Earth Science Reviews*, *174*, 84–121.

Wang, W. (Ed.) 2007. *Study on the coastal geomorphological sedimentation of the South China Sea*. Guangzhou, China. Guangdong Economy Publishing House (344 p. in Chinese).

Wang, Y., Cheng, H., Edwards, R., He, Y., Kong, X., An, Z., et al. (2005). The Holocene Asian Monsoon: Links to solar changes and North Atlantic climate. *Science*, *308*(5723), 854–857. https://doi.org/10.1126/science.1106296

Wei, G., Deng, W., Liu, Y., & Li, X. (2007). High-resolution sea surface temperature records derived from foraminiferal Mg/Ca ratios during the last 260 ka in the northern South China Sea. *Palaeogeography Palaeoclimatology Palaeoecology*, *250*, 126–138.

Wen, X., Liu, Z., Wang, S., Cheng, J., & Zhu, J. (2016). Correlation and anti-correlation of the East Asian summer and winter monsoons during the last 21,000 years. *Nature Communications*, *7*(1), 1–7. https://doi.org/10.1038/ncomms11999

Xia, D., Jia, J., Li, G., Zhao, S., Wei, H., & Chen, F. (2014). Out-of-phase evolution between summer and winter East Asian monsoons during the Holocene as recorded by Chinese loess deposits. *Quaternary Research*, *81*, 500–507.

Xie, S., Evershed, R., Huang, X., Zhu, Z., Pancost, R., Meyers, P., et al. (2013). Concordant monsoon-driven postglacial hydrological changes in peat and stalagmite records and their impacts on prehistoric cultures in central China. *Geology*, *41*, 827–830.

Yancheva, G., Nowaczyk, N., Mingram, J., Dulski, P., Schettler, G., Negendank, J., et al. (2007). Influence of the intertropical convergence zone on the East Asian monsoon. *Nature*, *445*(7123), 74–77. https://doi.org/10.1038/nature05431

Zhang, J., Bai, Y., Xu, S., Lei, F., & Jia, G. (2013). Alkenone and tetraether lipids reflect different seasonal seawater temperatures in the coastal northern South China Sea. *Organic Geochemistry*, *58*, 115–120.

Zhang, Y., Zhou, X., He, Y., Jiang, Y., Xie, Z., Sun, L., & Liu, Z. (2019). Persistent intensification of the Kuroshio Current during late Holocene cool intervals. *Earth and Planetary Science Letters*, *506*, 15–22.

Zhou, B., Zheng, H., Yang, W., Taylor, D., Lu, Y., Wei, G., et al. (2012). Climate and vegetation variations since the LGM recorded by biomarkers from a sediment core in the northern South China Sea. *Journal of Quaternary Science*, *27*, 948–955.